Kinetic separation of charge movement components in intact frog skeletal muscle

Christopher L.-H. Huang

Physiological Laboratory, Downing Street, Cambridge CB2 3EG, UK

1. Procedures for a complete charge movement separation employed a combination of its steady-state inactivation and activation properties in intact frog skeletal muscle fibres in gluconate-containing solutions.

2. Holding potential shifts from −70 to −50 mV reduced the total charge available between −90 and −20 mV from 16·76 ± 1·70 nC μF^{-1} (mean ± S.E.M.; $n = 4$ fibres) to 9·25 ± 1·43 nC μF^{-1} without significant loss of tetracaine-resistant charge (q_β).

3. The steady-state and kinetic properties of tetracaine-sensitive charge (q_γ) persisted through holding potential changes from −90 to −70 mV in the presence of gluconate and generally resembled activation properties established hitherto in sulphate-containing solutions.

4. Further holding potential displacement to −50 mV abolished q_γ charge movements and depressed the charge–voltage curve.

5. Test voltage steps applied from a −70 mV prepulse level gave rapid monotonic q_β decays and similarly depressed activation functions in 2 mM tetracaine unchanged by holding potential shifts between −70 and −50 mV.

6. The isolated 'on' q_γ charge movements, $I(t)$, always included early transients that preceded any prolonged charging phases and which increased with depolarization. They decayed to stable baselines in the absence of prolonged time-dependent or inward-current phases and yielded integrals, $Q(t)$, that monotonically increased with test voltage.

7. 'Off' steps always elicited rapid monotonic q_γ decays that fully returned the 'on' charge.

8. 'On' and 'off' q_γ currents, $I(t)$, following voltage steps from *fixed* conditioning to *varying* test levels mapped onto topologically distinct higher-order phase-plane trajectories, $I(Q)$, that steeply varied with test voltage.

9. In contrast, voltage steps to *fixed* test potentials of either −70 or −20 mV elicited *identical* q_γ phase-plane trajectories *independent* of prepulse history.

10. The q_γ current thus reflects an independent, capacitative process driven uniquely by higher-order dependences upon charge distribution, $Q(t)$, and test voltage, $V(t)$, autonomous of prepulse history or time, t.

Recent studies have established the tetracaine-sensitive (q_γ) charge movement component in the membrane of intact amphibian striated muscle. Its steep voltage sensitivity closely paralleled variations in intracellular Ca^{2+} release near threshold (Huang, 1981, 1990, 1993*a*; Hui, 1983; Irving, Maylie, Sizto & Chandler, 1989; Hui & Chandler, 1990). It was related to transitions in a dihydropyridine-sensitive voltage sensor localized selectively to the transverse tubules (Brum & Rios, 1987; Huang & Peachey, 1989; Huang, 1990). The remaining tetracaine-resistant (q_β) component exhibited a contrasting, more gradual, steady-state voltage dependence (Huang, 1982; Hui, 1983). However, such studies did not isolate the kinetic features of the q_γ currents as their experimental records also exhibited q_β charge movements (Adrian & Peres, 1979; Huang, 1982). Consequently, q_γ transients were clearly distinct as prolonged 'on' (>100 ms) decays or secondary 'humps' with further depolarization only at voltages near the contractile threshold (Adrian & Huang, 1984). They could not be distinguished either at larger depolarizations or at early times immediately following the application of test voltage steps (Huang, 1981).

Charge movements have recently been compared before and after particular pulse sequences or pharmacological

manipulations in cut fibres (Csernoch, Pizarro, Uribe, Rodriguez & Rios, 1991; Garcia, Pizarro, Rios & Stefani, 1991). These studies isolated a set of delayed 'on' transients followed by inward charging phases and biphasic 'off' responses which gave rise to 'on' and 'off' charge inequalities. These features together suggested that q_γ reflects electrical events secondary to intracellular Ca^{2+} release rather than charge movements driven primarily by voltage change (Pizarro, Csernoch, Uribe, Rodriguez & Rios, 1991; Szucs, Csernoch, Magyar & Kovacs, 1991). However, these studies predicted far smaller quantities of q_γ charge than reported elsewhere (Huang, 1982; Hui, 1983; Hui & Chandler, 1991). It was therefore possible that the observed difference traces actually reflected kinetic changes or small voltage shifts in an otherwise intact q_γ charge rather than the steady-state inactivation of a discrete intramembrane event (Csernoch *et al.* 1991; Hui, 1991; Jong, Pape & Chandler, 1992; Pape, Jong & Chandler, 1992).

The present study independently determined the steady-state inactivation and activation properties that were relevant to separation of q_γ currents in intact fibres in gluconate-containing solutions (Chen & Hui, 1991; Hui, 1991; Huang, 1994). Intact fibres consistently show late q_γ currents; this is not always the case in cut fibres (Adrian & Peres, 1979; Huang, 1981; cf. Melzer, Schneider, Simon & Szucs, 1986). They also permitted cable constants to be monitored through all experiments (Huang & Peachey, 1989). Particular holding, prepulse and test potential manoeuvres were developed to spare q_β charge, defined independently through both its tetracaine resistance and the effects of sustained depolarization (Huang, 1984; Hui & Chen, 1992). They thus isolated the q_γ charge movement and clarified several of its important features for the first time. Finally, a novel application of a phase-plane analysis suggested that q_γ charge movements reflect an independent, higher order, capacitative transition defined uniquely by charge distribution and test voltage.

METHODS

Sartorius muscles from cold adapted frogs (*Rana temporaria*), killed by pithing, were dissected in Ringer solution at 4–10 °C and stretched to a centre sarcomere length of 2·2–2·4 μm in a temperature-controlled recording chamber (Huang & Peachey, 1989). The extracellular solution was altered first to an isotonic tetraethylammonium-containing solution, and then to a hypertonic solution containing 500 mM sucrose after 10 min, both at 4–6 °C. The basic experimental solution comprised (mM): tetraethylammonium gluconate, 120; $MgCl_2$, 2; RbCl, 2·5; 3,4-diaminopyridine, 1; *N*-2-hydroxyethylpiperazine-*N'*-2-ethanesulphonic acid, 3; $CaCl_2$, 0·8; and 2×10^{-7} M tetrodotoxin buffered to pH 7·0 (see Huang, 1994). All experiments were performed within 2 h of introducing these external solutions.

A three-electrode voltage clamp of the pelvic ends of superficial muscle fibres directly accessible to the bathing solution (Adrian & Almers, 1976; Adrian, 1978) used 4–6 MΩ glass microelectrodes positioned at distances of $l = 375$ μm (voltage control electrode, V_1), $2l = 750$ μm (second voltage electrode, V_2) and $5l/2 = 940$ μm (current injection electrode, I_0), respectively from the fibre origin (Huang, 1981). Digital records of $V_1(t)$, $V_1(t) - V_2(t)$ and $I_0(t)$ were obtained at a 12-bit analog-to-digital conversion interval of 200 μs, after filtering to a 1 kHz cut-off frequency through 3-pole Butterworth filters, using a PDP 11/23 computer (Digital Equipment Corporation, Maynard, MA, USA) with a model 502 interface (Cambridge Electronic Design, Cambridge, UK). Unless otherwise stated in Results, five sweeps were averaged to constitute each test or control record. Linear fibre cable constants were determined from steady values of $V_1(t)$, $V_2(t)$ and the injected current, $I_0(t)$, at the end of depolarizing 30 mV control steps made to the −90 mV holding potential imposed 500 ms following a prepulse step to −120 mV. The membrane current through unit area of fibre surface with time t, ($I_m(t)$), was determined from calculated values of the fibre diameter, d, and internal sarcoplasmic resistivity, R_i:

$$I_m(t) = [V_1(t) - V_2(t)]\, d/(6l^2 R_i).$$

Charge movements were obtained from differences between test ($V_1 - V_2$) records and corresponding control records scaled appropriately to the ratio of the test and control voltage excursions. Control protocols with full cable analyses were interposed regularly between sets of five test voltages studied to verify fibre stability (Huang, 1990, 1991). Both test and control voltage steps lasted 124 ms. The capacitative charge, $Q(t)$, with time was computed using Simpson's rule after verifying complete current decays to stable DC levels (Adrian & Almers, 1974; Chandler, Rakowski & Schneider, 1976). Individual (unsubtracted) 'on' and 'off' test and control records were integrated after subtraction of templates derived from the scaling of the recorded (test or control) voltage (V_1) step by the ratio between the direct admittance current and the voltage excursion (Hui & Chandler, 1991; Huang, 1994). This precaution avoided leak admittance ambiguities caused by variations between test and control voltage clamp waveforms that would have affected direct integrations of difference records. The net (non-linear) charge transfer, $Q(t)$, was then deduced from comparisons of the appropriate test and control integration records.

Finally, alternate values of the isolated q_γ charge movements, $I(t)$, were plotted against the correponding net charge transfer, $Q(t)$, in the phase plane from the onset of the current transients to their full relaxation. The theory underlying such an analysis is described fully elsewhere (see Jordan & Smith, 1987). Briefly, this analysis yielded topological representations of the non-linear ordinary differential equations that could describe q_γ charge and gave indications of the kinetic order of the intramembrane charge movement. For example, one could so analyse first-order decays described by forward and backward voltage-dependent rate constants $k_1(V)$ and $k_{-1}(V)$:

$$dQ(t)/dt = k_1(V)Q(t) - k_{-1}(V)\{Q_{max} - Q(t)\}.$$

In the phase plane, this function becomes transformed into a straight line in which the time, t, is eliminated as an explicit variable:

$$dQ/dt = a_0(V) + a_1(V)Q.$$

The charge movement $I = dQ/dt$ is thus defined by the single-valued functions of voltage, $a_0(V)$ and $a_1(V)$. The latter are

formed from linear combinations of k_1 and k_{-1} which are themselves independent of the time, t, or charge, $Q(t)$. In contrast, departures from such linearity indicate a requirement for additional higher-order terms. In a virial series representation, these further contributions are similarly determined by further voltage-dependent coefficients $a_j(V)$:

$$I(t) = \Sigma a_j(V)[Q(t)]^j, \text{ where } j = 0, 1, 2 \ldots$$

The above expression represents a generalization of earlier representations of co-operative terms $O(Q^2..)$ that might influence the charge movement (see Huang, 1983, 1984).

$$dQ/dt = a_0(V) + a_1(V)Q + O(Q^2..).$$

A capacitative charge transfer would permit such a curved rather than linear phase-plane plot but would still require the charge movement, $I(t)$, to be determined uniquely by the test voltage V and the charge at that time, $Q(t)$. Hence, any given test voltage, V, should yield a unique phase-plane plot, $I(Q)$. The latter would occur only if the coefficients $a_j(V)$ are also autonomous of time t.

Results are given as means ± S.E.M.

RESULTS

Several of the above experimental measures proved essential for successful charge movement separation. The use of intact fibres permitted a full cable analysis not ordinarily available in cut fibre preparations (Irving, Maylie, Sizto & Chandler, 1987; Chandler & Hui, 1990). However, they require hypertonic extracellular solutions to suppress contraction, with possible consequences for tubular morphology. The Ca^{2+} replacement by Mg^{2+} and inclusion of both 3,4-diaminopyridine and tetraethylammonium in the bathing solutions minimized time-dependent ionic currents and enhanced identification of individual capacity contributions to charging records. Use of the anion substitute gluconate minimized Cl^- conductances and therefore the standing currents required to shift fibre holding potentials. This ensured preparations that remained stable through successive control cable analyses for even 1–2 h following electrode impalement (see figure legends).

Charge activation and inactivation shifted in directions that favoured q_β and q_γ charge separation in gluconate (see below). Charging currents were consistently outward in direction following 'on' (depolarizing) steps and inward following 'off' steps. The 'on' decays approached time-independent baselines without intervening inward phases or delayed slope currents. Sloping baseline corrections required by both control and test responses in some cut fibre preparations (Melzer *et al.* 1986) and by test responses in intact preparations (Adrian & Peres, 1979) thus proved unnecessary. This ensured unambiguous determinations of net capacitative charge. Finally, use of tetracaine sensitivity as a working definition of q_γ charge (Huang, 1981; Hui, 1983) resulted in steady-state charge separations in independent agreement with results from shifting the holding potential.

Differential charge inactivation between −70 and −50 mV in gluconate-containing solutions

The charge separation procedures required the charge inactivation characteristics of fibres exposed to gluconate. The relevant q_β and q_γ contributions were determined by exploring the effect of holding potential (V_h) on available charge both in the absence and in the presence of 2 mM tetracaine. The test pulses were imposed after 500 ms following prepulse steps that returned the membrane potential to a level of −90 mV. They were made to a test potential of −20 mV, and therefore represented a voltage excursion that would normally transfer both q_β and q_γ charge (Huang, 1984). Holding potentials were incremented in 10 mV steps between −90 and −20 mV, with each run of test steps beginning at least 30 s following each shift (Fig. 1*A*, inset). The bracketing control steps employed a holding potential consistently restored to −90 mV. Additional bracketing controls were also made at each of the holding potentials studied to assess for changes consequent upon any charge interconversion associated with inactivation.

Figure 1 plots the resulting charge movement, Q_{max}, against holding potential, V_h, in 0 mM (*A a*) and 2 mM tetracaine (*A b*). Use of the anion substitute gluconate gave rise to the following features useful for q_γ charge separation. First, maximum charge was diminished even in fully polarized fibres ($Q_{max} = 17{\cdot}30 \pm 1{\cdot}41$ nC μF^{-1} in four fibres at $V_h = -90$ mV; Fig. 1*A a*) relative to corresponding values from similar preparations in sulphate-containing media (around 28–30 nC μF^{-1}; Huang, 1982). This reduction preferentially involved q_β charge which fell to $8{\cdot}18 \pm 0{\cdot}91$ nC μF^{-1} (5 fibres; cf. Chen & Hui, 1991 concerning cut fibres). This minimized the net q_β charge contributions in the isolation manoeuvres below.

Second, holding potential shifts from −90 to −70 mV altered neither total steady-state charge (Fig. 1*A a*) nor the corresponding charge movements (Fig. 1*B*). Both holding levels yielded the rapid decays expected from a combination of monotonic q_β currents and the rapid q_γ transients expected with large depolarizing steps (Adrian & Peres, 1979; Huang, 1982). However, a further holding potential shift to −50 mV significantly inactivated the available charge from $16{\cdot}77 \pm 1{\cdot}76$ to $9{\cdot}26 \pm 1{\cdot}43$ nC μF^{-1} ($n = 4$ fibres; Fig. 1*A a*, double-headed arrows) and reduced charge movements (Fig. 1*B*).

Third, the q_β charge movements that persisted in 2 mM tetracaine gave rise to reduced inactivation functions (Fig. 1*A b*). These declined considerably more gradually with holding potential in gluconate than reported in sulphate (cf. Huang, 1984). Thus, holding potential shifts from −70 to −50 mV only minimally affected available charge. The dip in the overall inactivation function in Fig. 1*A a* therefore represents a preferential inactivation of q_γ over q_β charge, provided q_γ is defined through its selective sensitivity to millimolar tetracaine concentrations.

However, the two sets of data points (Fig. 1*A a* and *A b*) next merged with further depolarization reflecting a sole contribution from q_β inactivation.

Finally, Fig. 1*A c* plots the charge movement in response to control-type voltage steps at varying holding potentials. The non-linear charge is normalized to values obtained in fully polarized muscle fibres. Charge inactivation was not accompanied by detectable interconversions into extra charge in the control voltage range (cf. Brum & Rios, 1987; Huang, 1993*b*).

Divergence of q_β and q_γ charge activation functions in gluconate beyond −60 mV

Figure 2 compares q_β and q_γ charge–voltage (activation) curves obtained whilst stepping individual fibres through holding potential values between −90 and −50 mV as prompted by the above inactivation data. The pulses to the test voltages, V, followed 500 ms after prepulses to a fixed, −90 mV, conditioning level. This also yielded features that would optimize q_γ charge separation in the presence of gluconate. First, there was the marked increase in steady-state charge associated with the q_γ threshold but this was shifted to around −60 mV in gluconate from the approximately −45 mV threshold reported hitherto in sulphate-containing solutions (Fig. 2*A*; Huang, 1982). Voltage steps made from a fully polarized membrane potential hence would transfer enhanced q_γ relative to q_β charge. Nevertheless, the charge–voltage curves retained the two-component form reported earlier in both intact and cut preparations (Adrian & Almers, 1976; Huang, 1982; Hui & Chandler, 1990).

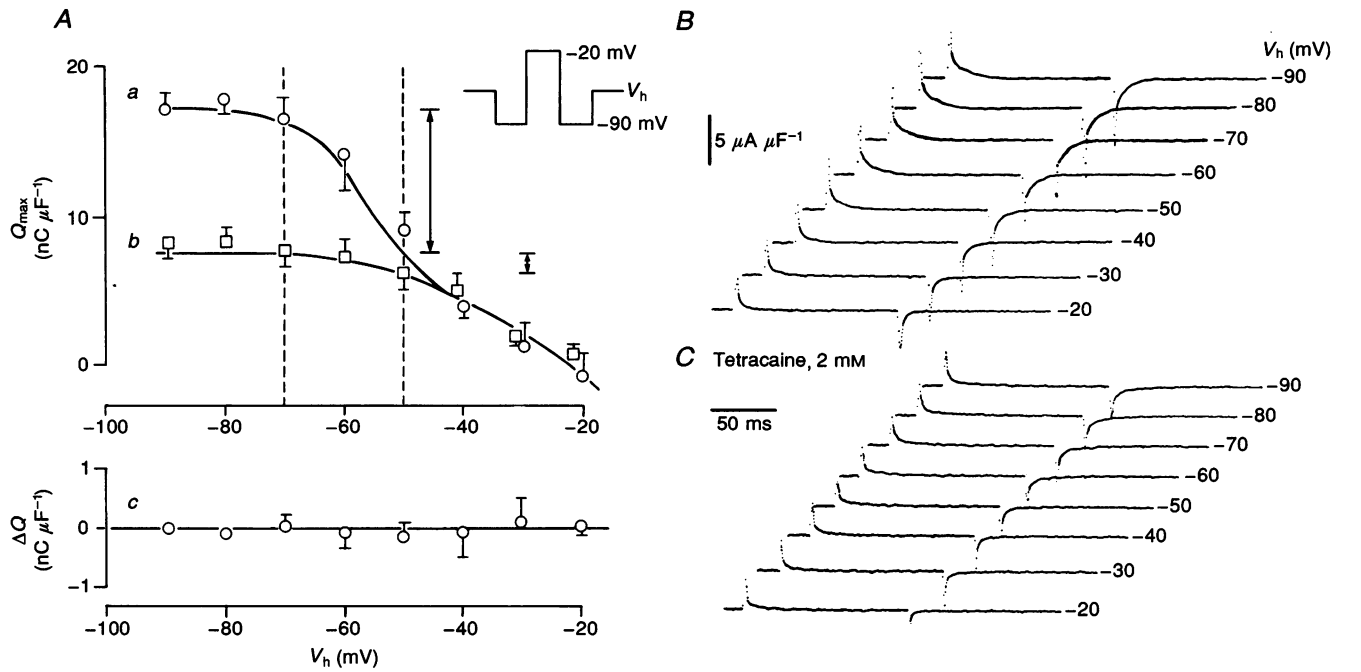

Figure 1. Inactivation of charge movement components in gluconate
Charge inactivation curves (*A a* and *A b*) and representative charge movements (*B* and *C*) in gluconate-containing bathing solutions determined by voltage clamp steps from a −90 mV prepulse level to a fixed test voltage of −20 mV (lines drawn by eye). Data obtained in the absence (*A a* and *B*) and the presence (*A b* and *C*) of 2 mM tetracaine. *A a*, four fibres (designations: V57, V58, V63 and V68) studied in the absence of tetracaine at 2·7 ± 0·52 °C. Specific cable constants (means ± S.E.M.) at outset of experiments: $d = 69{\cdot}5 \pm 5{\cdot}17$ μm, $R_m = 6{\cdot}55 \pm 1{\cdot}12$ kΩ cm^2, and $C_m = 6{\cdot}6 \pm 0{\cdot}44$ μF cm^{-2}. At end of test procedures: $d = 71{\cdot}8 \pm 7{\cdot}65$ μm, $R_m = 6{\cdot}21 \pm 1{\cdot}11$ kΩ cm^2, and $C_m = 7{\cdot}3 \pm 0{\cdot}44$ μF cm^{-2}. *A b*, five fibres (designations: V77, V79, V80, V81, V82) studied in 2 mM tetracaine at a temperature of 5·5 ± 0·1 °C. Initial cable constants: $d = 79{\cdot}9 \pm 10{\cdot}74$ μm, $R_m = 5{\cdot}57 \pm 0{\cdot}92$ kΩ cm^2, and $C_m = 5{\cdot}5 \pm 0{\cdot}64$ μF cm^{-2}. At end of procedures: $d = 78{\cdot}2 \pm 10{\cdot}7$ μm, $R_m = 4{\cdot}30 \pm 0{\cdot}56$ kΩ cm^2, and $C_m = 6{\cdot}6 \pm 0{\cdot}99$ μF cm^{-2}. *A c*, charge movements in response to voltage steps between −120 and −90 mV at different holding potentials in comparison to the charge moved by the same voltage step at a −90 mV holding potential. *B* and *C*, charge movements in response to voltage steps between a −90 mV prepulse level and a constant test voltage of −20 mV at different holding potentials, V_h. *B*, fibre V58 in the absence of tetracaine; temperature, 1·5 °C. Initial cable constants: $d = 80{\cdot}7$ μm, $R_m = 8{\cdot}04$ kΩ cm^2, and $C_m = 7{\cdot}8$ μF cm^{-2}. Following pulse procedures: $d = 87{\cdot}1$ μm, $R_m = 7{\cdot}58$ kΩ cm^2, and $C_m = 8{\cdot}5$ μF cm^{-2}. *C*, fibre V80 in 2 mM tetracaine; temperature, 5·7 °C. Initial cable constants: $d = 101{\cdot}9$ μm, $R_m = 6{\cdot}84$ kΩ cm^2, and $C_m = 6{\cdot}3$ μF cm^{-2}. Final cable constants: $d = 98{\cdot}3$ μm, $R_m = 5{\cdot}34$ kΩ cm^2, and $C_m = 7{\cdot}1$ μF cm^{-2}.

Second, holding potential shifts from −90 to −70 mV did not affect the charge–voltage curve. Clear 'on' q_γ charge transfers were observed at test potentials of −45 and −55 mV even with sustained depolarization to −70 mV (Fig. 2*B*; see dashed lines in Fig. 2*A*). Thus q_γ activation is normal under these conditions. Third, a further shift in holding voltage to −50 mV reduced the charge–voltage curve particularly beyond a test voltage of −60 mV (Fig. 2*A*). It left an activation function that resembled the voltage dependence of tetracaine-resistant (q_β) charge (see below; cf. Huang, 1982; Hui, 1983) and abolished the prolonged 'on' q_γ charge movements to leave exponential q_β decays (Fig. 2*B*).

Persistence of q_β charge through the separation protocols

The above findings provided a basis for the complete isolation of q_γ charge movement in gluconate-containing solutions. This imposed test voltage steps from a prepulse level of −70 rather than the more usual −90 mV in order to maximize the extent of q_γ relative to q_β charge transfer. The resulting records obtained at a holding potential of −70 mV (rather than −90 mV) were compared with the corresponding traces that followed prolonged depolarization to −50 mV; the latter preferentially inactivated q_γ charge. This procedure was first tested on fibres exposed to

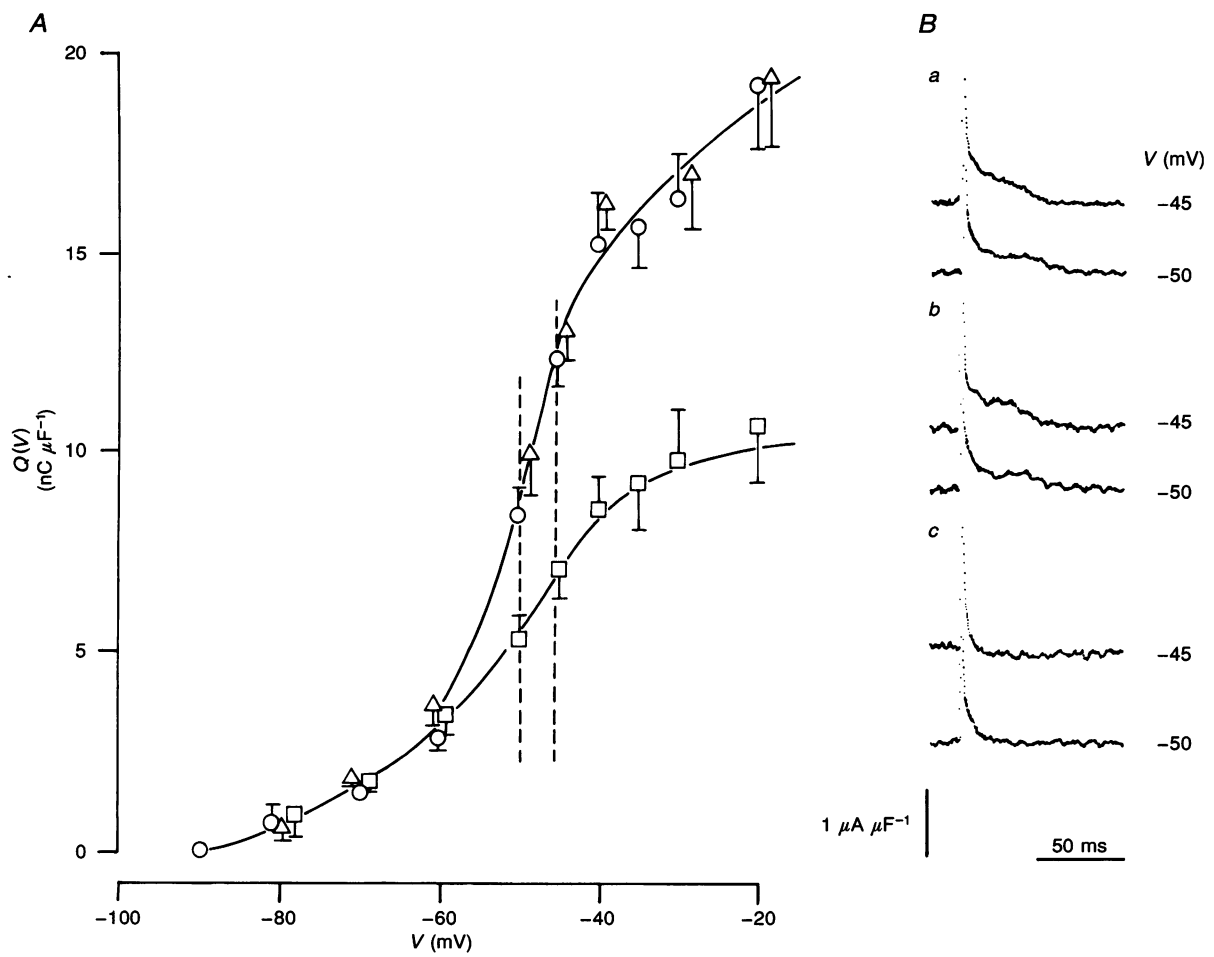

Figure 2. Charge activation properties and their divergence with holding potential changes in gluconate-containing solutions

A, charge–voltage curves from seven fibres (designations V54–58, V64–66; lines drawn by eye) studied at holding potentials of −90 mV (△); −70 mV (○); and −50 mV (□), respectively; temperature, 2·92 °C. Initial cable constants: $d = 71{\cdot}0 \pm 6{\cdot}86$ μm, $R_m = 8{\cdot}82 \pm 2{\cdot}62$ kΩ cm², and $C_m = 6{\cdot}8 \pm 0{\cdot}39$ μF cm^{-2}. Final cable constants: $d = 72{\cdot}9 \pm 6{\cdot}69$ μm, $R_m = 8{\cdot}13 \pm 2{\cdot}42$ kΩ cm², and $C_m = 7{\cdot}9 \pm 0{\cdot}60$ μF cm^{-2}. *B*, charge movements elicited by voltage steps from a prepulse level of −90 mV to test levels of −50 and −45 mV, respectively, at successive holding levels of −90 mV (*Ba*); −70 mV (*Bb*); and −50 mV (*Bc*) to demonstrate the inactivation of delayed q_γ charge. Fibre V55; temperature, 3·6 °C. Initial cable constants: $d = 103{\cdot}7$ μm, $R_m = 24{\cdot}96$ kΩ cm², and $C_m = 6{\cdot}5$ μF cm^{-2}. Following experimental procedures: $d = 100{\cdot}8$ μm, $R_m = 22{\cdot}94$ kΩ cm², and $C_m = 6{\cdot}1$ μF cm^{-2}.

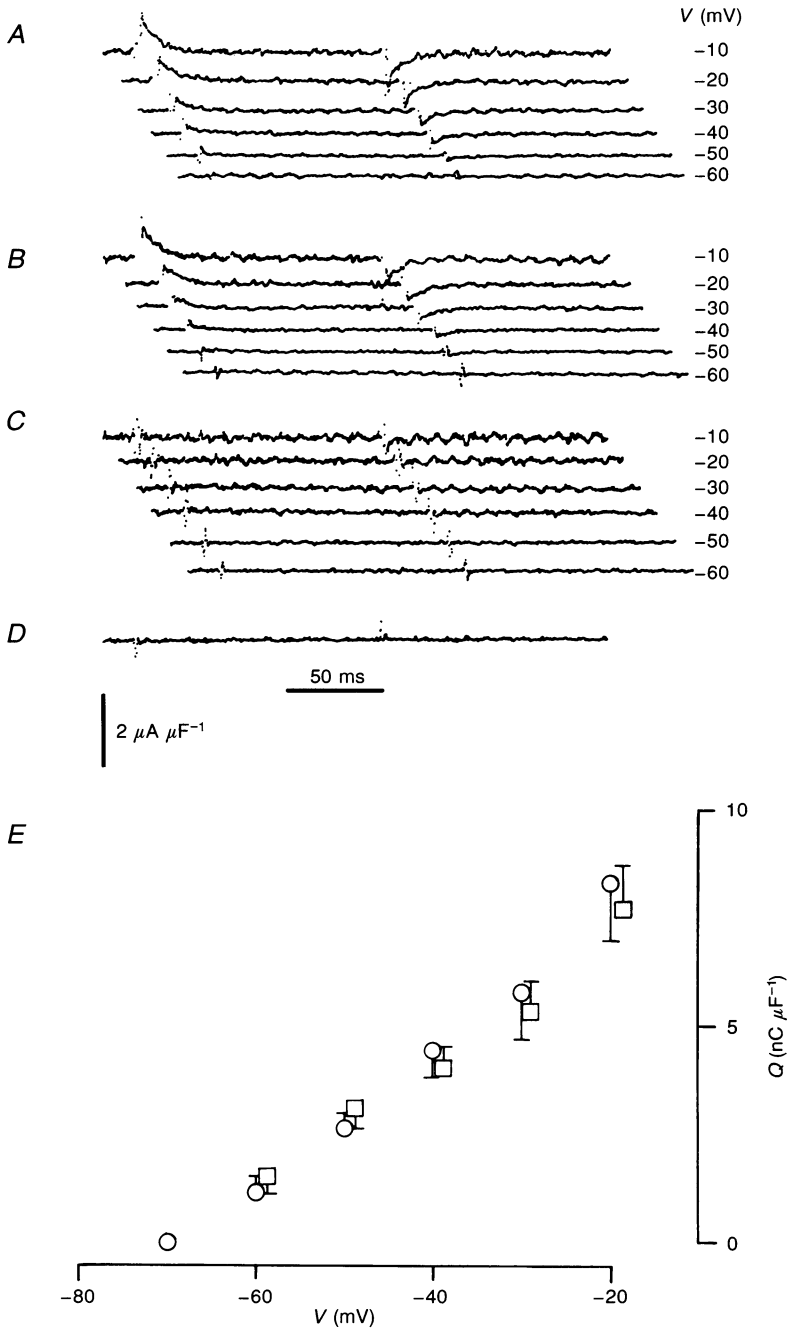

Figure 3. The charge separation procedure applied to tetracaine-treated fibres
A and *B*, typical charge movement records in fibres in 2 mM tetracaine following a range of depolarizing steps from a fixed prepulse level of −70 mV and holding potentials of −70 mV (*A*) and −50 mV (*B*), respectively. *C*, traces obtained from the difference (*A* − *B*). *D*, difference trace obtained by comparing the bracketing control currents following, and prior to, the above manoeuvres. Fibre V79; temperature, 5·50 °C. Initial cable constants: $d = 56{\cdot}9\ \mu m$, $R_m = 10{\cdot}11\ k\Omega\ cm^2$, and $C_m = 2{\cdot}6\ \mu F\ cm^{-2}$. Final cable constants: $d = 53{\cdot}9\ \mu m$, $R_m = 7{\cdot}95\ k\Omega\ cm^2$, and $C_m = 2{\cdot}9\ \mu F\ cm^{-2}$. *E*, transfer of tetracaine-resistant charge at the −70 mV (○) and −50 mV (□) holding potentials. Six fibres (designated V75–V80); temperature, 5·4 ± 0·1 °C. Initial cable constants: $d = 93{\cdot}8 \pm 12{\cdot}3\ \mu m$, $R_m = 9{\cdot}14 \pm 0{\cdot}79\ k\Omega\ cm^2$, and $C_m = 7{\cdot}1 \pm 1{\cdot}32\ \mu F\ cm^{-2}$. Cable constants following procedures: $d = 90{\cdot}0 \pm 13{\cdot}02\ \mu m$, $R_m = 6{\cdot}88 \pm 0{\cdot}45\ k\Omega\ cm^2$, and $C_m = 7{\cdot}9 \pm 1{\cdot}67\ \mu F\ cm^{-2}$.

2 mM tetracaine to exclude significant effects on q_β charge (Huang, 1981; Hui, 1983). Figure 3*A* displays such q_β charge movements in response to depolarizing test voltage steps. The monotonic decays obtained increased in amplitude with progressive depolarization but were not followed by q_γ transients. The corresponding records at a shifted, −50 mV, holding potential (Fig. 3*B*) were obtained using test steps superimposed 500 ms following a pulse to the same −70 mV prepulse level. They showed no significant qualitative or quantitative differences in magnitude or form from q_β currents obtained in the more polarized fibres. Thus, the corresponding pairs of records (*A* − *B*) yielded flat difference traces (Fig. 3*C*). Comparisons of control traces acquired at the end and at the outset of the experiment also gave flat difference records and so confirmed preparation stability through each experiment (Fig. 3*D*).

The corresponding charge–voltage curves (means ± S.E.M.; Fig. 3*E*) were depressed as expected for fibres in 2 mM tetracaine. However, they now remained constant in the face of holding potential shifts from −70 to −50 mV and displayed similar displacements of non-linear charge (8–9 nC μF^{-1}) over the available voltage range (−70 to −20 mV). Hence, the use of this holding potential change and of millimolar tetracaine concentrations would independently accomplish concordant separations of q_β and q_γ charge (see Discussion). The experimental manoeuvres adopted here would therefore achieve a

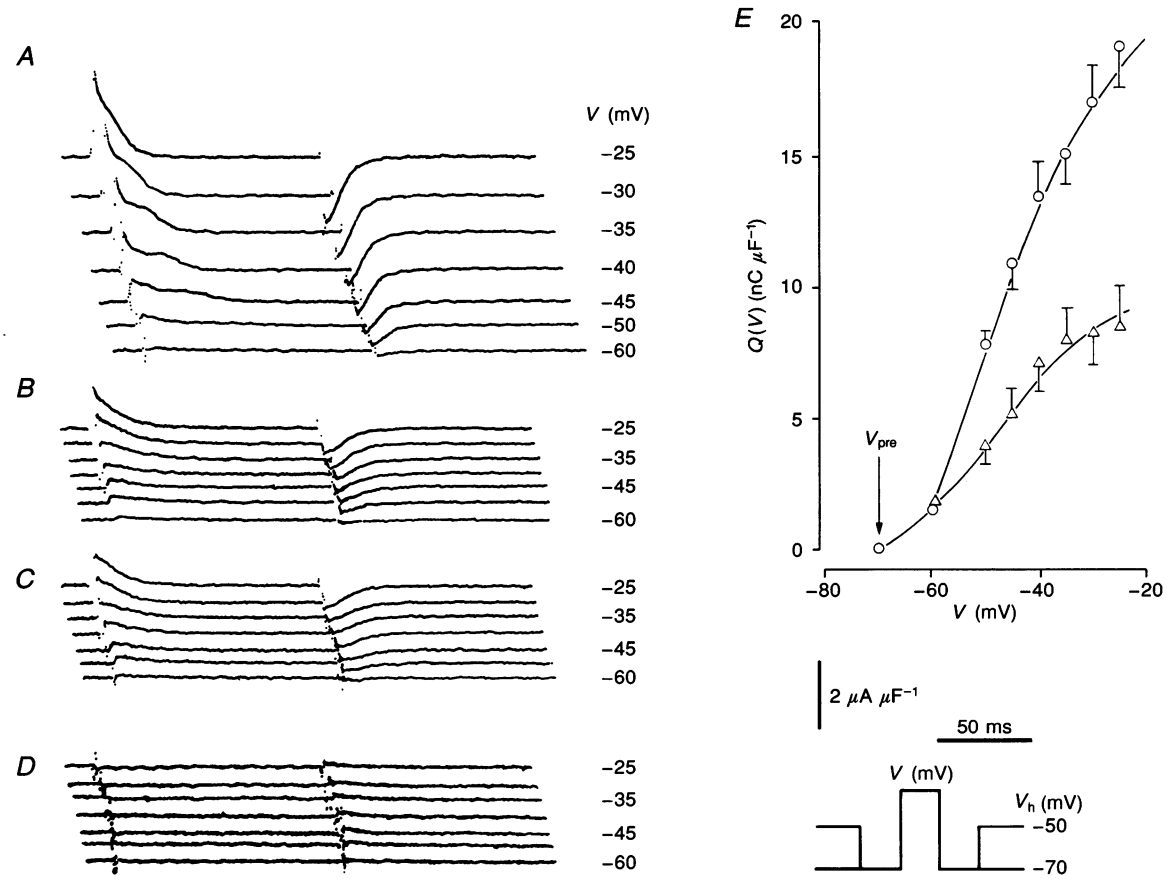

Figure 4. The charge separation procedure applied to the isolation of q_γ charge
A–C, charge movements at the holding voltages of −70 mV (*A*) and at −50 mV (*B* and *C*) before (*B*) and after (*C*) shifting the holding voltage from −50 to −70 mV. *D*, difference traces (*B* − *C*) generated from corresponding records in *B* and *C*. *A–C*, fibre V70; temperature, 5 °C. Initial cable constants: $d = 50{\cdot}7\ \mu m$, $R_m = 4{\cdot}64\ k\Omega\ cm^2$, and $C_m = 4{\cdot}4\ \mu F\ cm^{-2}$. Final cable constants: $d = 48{\cdot}4\ \mu m$, $R_m = 3{\cdot}76\ k\Omega\ cm^2$, and $C_m = 4{\cdot}4\ \mu F\ cm^{-2}$. *E*, charge moved by a range of depolarizing steps from a fixed prepulse level of −70 mV and holding potentials of −70 mV (○) and −50 mV (△), respectively, in the absence of tetracaine (lines drawn by eye). Four fibres (designated V68–71) studied in *E*; temperature, 4·5 ± 0·43 °C. Initial cable constants: $d = 58{\cdot}5 \pm 3{\cdot}54\ \mu m$, $R_m = 5{\cdot}36 \pm 0{\cdot}83\ k\Omega\ cm^2$, and $C_m = 5{\cdot}7 \pm 0{\cdot}58\ \mu F\ cm^{-2}$. Following the test procedures: $d = 60{\cdot}5 \pm 3{\cdot}9\ \mu m$, $R_m = 5{\cdot}36 \pm 0{\cdot}76\ k\Omega\ cm^2$, and $C_m = 6{\cdot}2 \pm 0{\cdot}65\ \mu F\ cm^{-2}$.

selective isolation of q_γ charge movements with minimal contamination from changes in either the kinetics or the steady-state distribution of q_β charge.

The extraction of q_γ charge movement

The above extraction procedure for q_γ charge movement was next applied to fibres exposed to gluconate but not to tetracaine (Fig. 4). Heavily signal averaged (10 sweeps per average) charge movements were obtained at a −50 mV holding potential, following its shift to −70 mV and after its final return to −50 mV (Fig. 4*A–C*). Application of small depolarizing steps yielded monotonic q_β decays in fully polarized fibres. However, larger depolarizations both increased the amplitude of the early decays and brought on prolonged q_γ transients (>100 ms), in contrast to the observations in tetracaine-treated fibres at a −70 mV holding potential. The delayed currents became both larger and more rapid with even small (10–20 mV) further depolarization (Fig. 4*A*). However, fibres at a holding potential of −50 mV showed q_β decays alone whether before (Fig. 4*B*) or after (Fig. 4*C*) the change in holding level. Corresponding pairs (*C* − *B*) in the latter set of traces gave flat difference records (Fig. 4*D*) confirming fibre stability through and effective bracketing of the experimental procedure.

The corresponding charge–voltage curves agreed with findings resulting from the use of the more usual conditioning level of −90 mV. In particular, holding potential shifts to −50 mV (Fig. 4*E*) reduced both the magnitude and steepness of the charge–voltage function, particularly beyond a test potential of −60 mV, even when tetracaine was absent. Yet it left a voltage dependence identical to that obtained in 2 mM tetracaine (Fig. 3*E*). This reinforces the finding, indicated in the previous section, that holding potential changes between −70 and −50 mV and treatment with millimolar tetracaine separately achieve identical q_β and q_γ fractionations in the steady state.

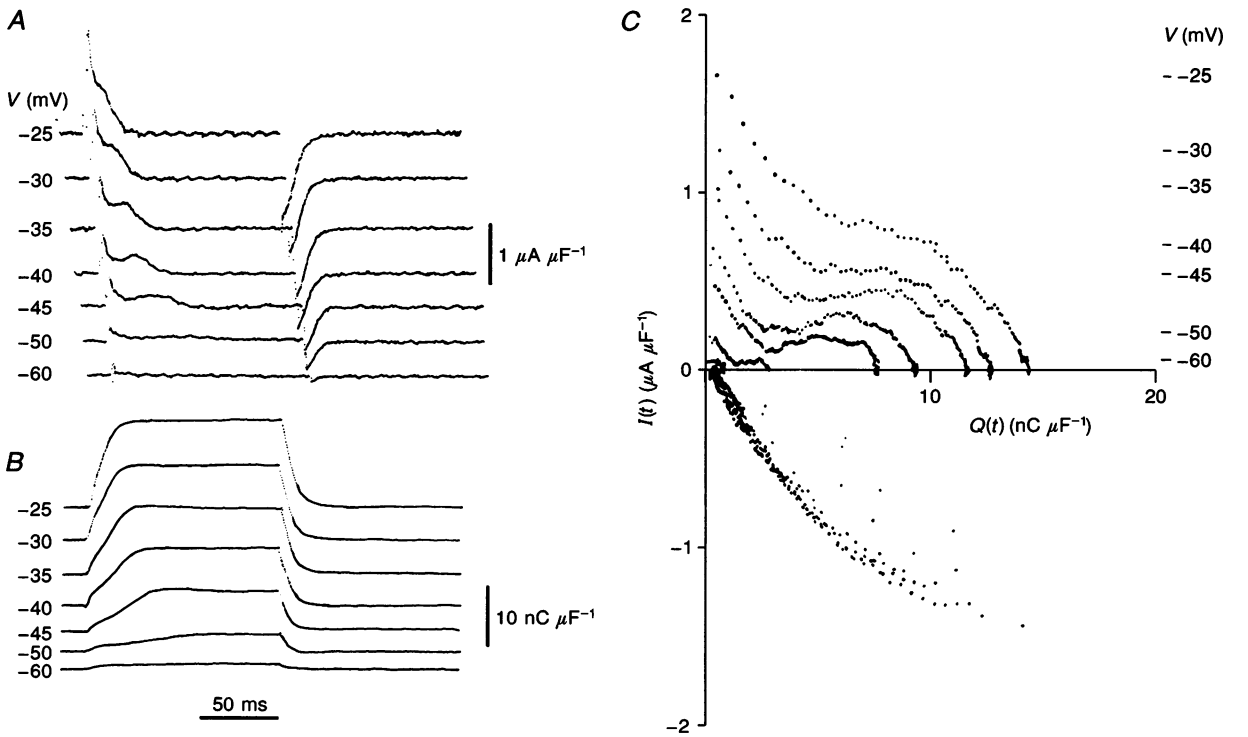

Figure 5. Phase-plane analysis of q_γ charge movements at different test voltages
A, records obtained through subtractions of charge movements obtained at a holding potential of −50 mV from records obtained at a −70 mV holding potential, to separate q_γ charge movement. The relevant traces were obtained through the imposition of depolarizing steps to a range of test potentials from a constant, −70 mV, prepulse level. *B*, running integrals obtained by the application of Simpson's rule to the separate transients to demonstrate overall conservation of charge. *C*, phase-plane representations of the 'on' (upper) and 'off' (lower) responses of the q_γ intramembrane charge to applied voltage steps plotting the charge movement $I(t)$ against the charge $Q(t)$. Fibre V70; cable constants and temperature listed in legend to Fig. 4.

Features of isolated q_γ currents

The full time course of q_γ currents was next obtained by subtracting currents obtained at a −50 mV holding potential from those obtained at the same test potentials but a holding potential of −70 mV. Figure 5*A* establishes a number of features of this isolated q_γ charge movement for the first time. First, prolonged transients with complex charging waveforms were prominent over a broader voltage range, over −50 to −30 mV, than demonstrated hitherto (Adrian & Peres, 1979; Huang, 1982). Second, a significant and rapid early q_γ current always immediately followed the 'on' voltage step (< 5 ms). These early 'on' currents increased in magnitude with depolarization. This suggested an underlying intramembrane charge whose distribution then would deviate most from its appropriate steady-state value immediately after the step. Third, the 'off' steps elicited prominent monotonic q_γ decays and not the complex waveforms reported in cut fibres (Csernoch *et al.* 1991). These similarly scaled with voltage excursion. Fourth, both the 'on' and the 'off' q_γ decays reached steady baselines without any intervening outward current slopes or transient inward charging phases, contrary to earlier reports in cut fibres (Csernoch *et al.* 1991; Garcia *et al.* 1991; Pizarro *et al.* 1991).

Finally, q_γ charge was conserved through all 'on' and 'off' steps as expected from an intramembrane charge as opposed to other current sources. This also contrasted with the earlier reports (Szucs *et al.* 1991). Running integrals of q_γ charge thus tended asymptotically towards steady values which increased with depolarization and returned to the baseline with the end of the step (Fig. 5*B*).

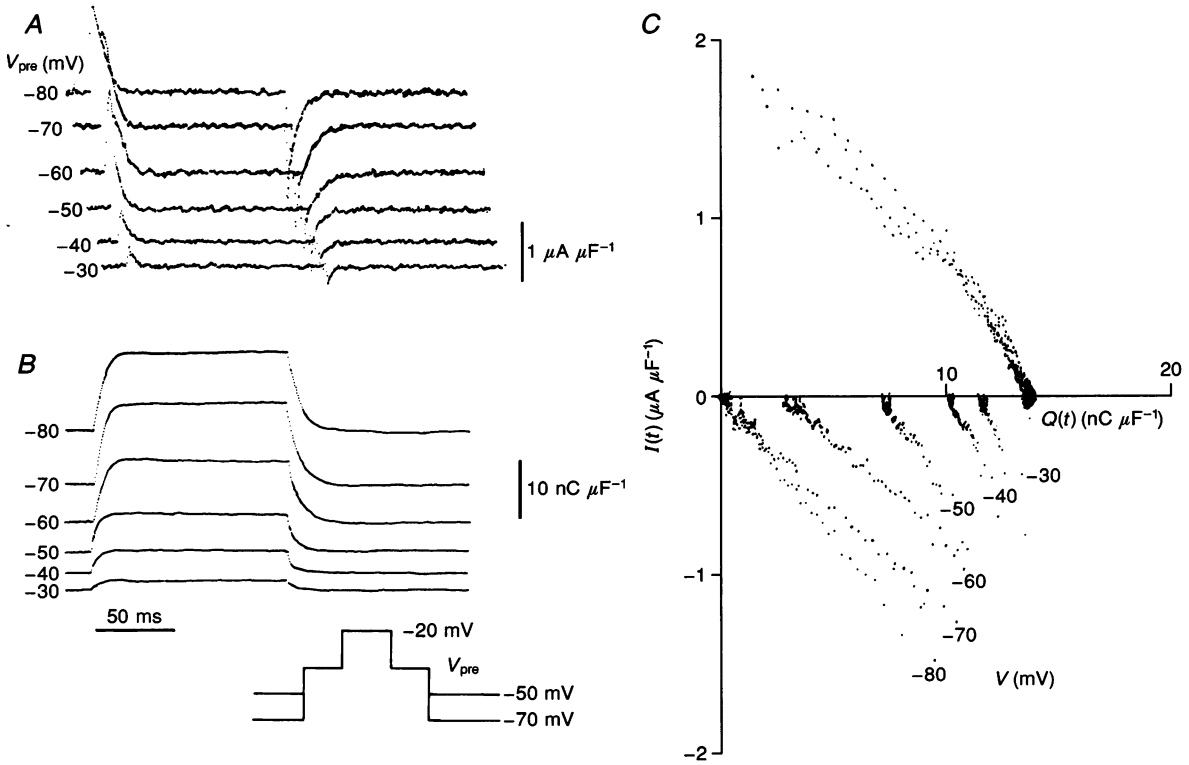

Figure 6. Phase-plane analysis of q_γ charge movements; varying prepulse but fixed test voltages

A, records obtained through subtraction of charge movements obtained at a holding potential of −50 mV from records obtained at a −70 mV holding potential to separate q_γ charge movement. The relevant traces were obtained through the imposition of depolarizing steps from varying prepulse potentials to a fixed −20 mV test pulse level (see inset). *B*, running integrals obtained by the application of Simpson's rule to the separate transients. *C*, phase-plane representations of the 'on' (upper) and 'off' (lower) responses of the q_γ intramembrane charge to applied voltage steps plotting the charge movement $I(t)$ against the charge $Q(t)$ as plotted relative to the charge movement at −20 mV. Fibre V63; temperature 4·2 °C. Cable constants at outset: $d = 56{\cdot}5\ \mu m$, $R_m = 5{\cdot}048\ k\Omega\ cm^2$, and $C_m = 5{\cdot}27\ \mu F\ cm^{-2}$. Following experimental procedures: $d = 52{\cdot}6\ \mu m$, $R_m = 4{\cdot}57\ k\Omega\ cm^2$, and $C_m = 5{\cdot}77\ \mu F\ cm^{-2}$.

Phase-plane analysis of isolated q_γ charge movements

The complex nature and steep voltage dependence of q_γ waveforms were not amenable to explicit analytical representation. Nevertheless, the averaged current records, $I(t) = dQ/dt$ (Fig. 5*A*), could be plotted against the corresponding charging, $Q(t)$, records (Fig. 5*B*) in the phase plane. This offered an empirical topological representation of the differential equations that describe q_γ charge movement at different test voltages (V) for the first time. The description assumed a form autonomous of the time t that followed the imposition of the 'on' or 'off' voltage steps (Kreyszig, 1976; Jordan & Smith, 1987).

Figure 5*C* (upper panel) displays phase-plane transformations of responses to 'on' steps made from a *fixed* prepulse level of −70 mV to test voltages which *varied* between −25 and −60 mV. These plots were compatible with capacitative transitions varying steeply with membrane potential and charge distribution albeit through higher order mechanisms. First, each trajectory, $I(Q)$, began from a maximum value appropriate to the steady charge, Q, expected at the prepulse potential. Second, it was complex in form and so excluded a first-order process that would map onto a linear function in the phase plane. Third, both the shape and magnitude of the plots varied with both the charge, Q, on the abscissa and the test voltage, V. The loci deviated most from linearity between testing voltages of −45 and −35 mV, where they showed two turning points requiring at least two higher-order terms in any underlying rate equation (see Methods for theory). However, they became smoother and tended towards linearity with further depolarization. Fourth, they ended at stable critical points on the abscissa that corresponded to the expected value of steady-state charge at V.

Finally, the lower panel of Fig. 5*C* examines 'off' responses to steps from varying 'on' test voltages returning to the fixed recovery voltage of −70 mV. These loci began from different values of the charge $Q(t)$ appropriate to the 'on' charge moved by the preceding test step. Nevertheless, all the experimental points converged to a single function accordingly independent of the different charging histories. The loci ended at a single origin that corresponded to zero net 'off' charge transfer and, therefore, a net charge conservation whatever the 'on' test potential. This convergence to a single locus implies that the q_γ current, $I(t)$, was uniquely determined by the 'off' voltage and the charge at time t, $Q(t)$, and was independent of previous charging 'on' history.

Isolated q_γ charge movements at depolarized test potentials

Previous studies have not attempted a separation of q_γ charge movements following large depolarizing steps as these produced an extensive overlap between q_β and q_γ waveforms. The final experiments isolated the q_γ charge movement in response to steps imposed from prepulse voltages which varied between −30 and −80 mV. These were made to a depolarized but fixed test potential of −20 mV (Fig. 6, inset). Figure 6*A* demonstrates persistent q_γ charge movements even with such large depolarizations, but these took the form of monotonic 'on' and 'off' currents (Fig. 6*A*) whose amplitude and integrals (Fig. 6*B*) increased with the size of the depolarizing step. They also declined to steady current pedestals without showing either inward-current phases or delayed time-dependent currents. These features contrast with the decline in the amplitude achieved by q_γ currents reported in cut fibres at large depolarizations (Pizzaro *et al.* 1991). Finally, 'on' and 'off' charge movement was conserved at all prepulse voltages (Fig. 6*B*).

The corresponding 'on' phase-plane trajectories (Fig. 6*C*, upper panel) began at values of charge Q that varied with prepulse voltage. They ended at a single nodal point on the abscissa appropriate to the steady-state q_γ charge movement at the fixed test voltage of −20 mV. Nevertheless, all the loci converged to a common trajectory independent of the varying charging histories. Conversely, the 'off' loci converged to different nodal points and with different slopes that varied with the prepulse voltage, V, to which the potential returned after the step (Fig. 6*C*, lower panel).

The complementary findings arising from fixed prepulse and varied test pulse voltages were consistent with a charge movement, $I(t)$, that obeyed a steep and higher-order dependence upon test voltage, V, and the charge distribution $Q(t)$ at that time t. The findings arising from experiments that instead varied the prepulse voltage were consistent with an $I(Q)$ dependence autonomous of previous charging history, also as expected for an intramembrane capacitative charge.

DISCUSSION

This study optimized the separation of q_β and q_γ charge movements in intact striated muscle through the application of independently determined steady-state activation and inactivation characteristics. Earlier reports resolved the individual components in the steady state but did not isolate their respective kinetic properties (Huang, 1982; Hui, 1983; Huang & Peachey, 1989; Huang, 1990). They identified delayed q_γ 'hump' currents over a narrow threshold voltage range in intact fibres (Adrian & Huang, 1984). However, the q_γ and q_β decays markedly overlapped both at larger depolarizations and at early times following the imposition of voltage steps (Adrian & Peres, 1979; Huang, 1982). Furthermore, even the delayed q_γ currents occurred inconsistently in experimental records from some cut fibre preparations (Melzer *et al.* 1986).

Recent procedures compared charge movements before and after particular manipulations in cut fibres (Csernoch, *et al.* 1991; Garcia *et al.* 1991). They isolated a delayed 'on' current followed by an inward charging phase which showed biphasic 'off' responses and resulted in an 'on'–'off' charge inequality. These traces were identified with a q_γ transient secondary to intracellular Ca^{2+} release (Pizarro *et al.* 1991; Szucs *et al.* 1991). However, they predicted a far smaller quantity of q_γ charge than reported in intact fibres (Huang, 1982; Hui, 1983; Hui & Chandler, 1991). It was also possible that the observed difference traces reflected kinetic changes or small voltage shifts in an otherwise intact q_γ charge, rather than the actual steady-state inactivation of a discrete process, whatever its mechanism (Csernoch *et al.* 1991; Hui, 1991; Jong *et al.* 1992; Pape *et al.* 1992).

The present experiments modified the existing procedures used previously in either intact or cut fibres (Huang, 1984; Csernoch *et al.* 1991) while avoiding repetitive electrode impalements or external solution changes. They adopted conditions that facilitated identification of capacity currents and minimized ionic and standing leak currents. Cable constant verifications could be intercalated through each experiment in intact fibres to confirm their stability and the integrity of the control current records. The q_γ charge was defined in terms of its sensitivity to millimolar tetracaine concentrations. Earlier reports indicated that this yielded charge separations that agreed with kinetic criteria (Hui, 1983), the results of steady-state analyses using double Boltzmann functions (Hui & Chandler, 1990) and with 'off' charge separations in two-step protocols in cut fibres (Hui & Chen, 1992). The findings here further confirmed that such a separation agreed with independent results from applying holding potential shifts between −70 and −50 mV in intact fibres exposed to gluconate.

The charge separation procedure compared capacity currents before and after simple manoeuvres of holding and test potential. It was facilitated by some additional effects of gluconate. Thus, gluconate preferentially reduced steady-state q_β charge (cf. Chen & Hui, 1991) and gave flat q_β inactivation functions particularly between holding potentials of −70 and −50 mV in contrast to the maximal q_γ inactivation achieved under identical conditions. Similar manoeuvres would have inactivated both q_β and q_γ charge in sulphate-containing solutions (Huang, 1984). Gluconate also selectively shifted the q_γ activation curve to voltage regions in which there was minimal q_β charge movement and so offered a prepulse voltage condition that would preferentially transfer q_γ charge. A final test of the resulting separation protocol excluded influences on the kinetic or steady-state properties of q_β charge.

The charge separation procedure was based accordingly on independently established steady-state activation and inactivation properties for the q_γ system. It therefore isolated charging currents that reflected a discrete component of steady-state q_γ charge and not merely an alteration in its kinetics (Csernoch *et al.* 1991; Jong *et al.* 1992; Pape *et al.* 1992).

Several properties of q_γ charge movement have now been clarified directly for the first time. First, significant q_γ charge movement commenced immediately following 'on' voltage steps, cotemporal with early q_β charge movements. This suggests a causally independent q_γ capacity decay driven directly by charge distribution and voltage rather than a sequel to q_β charge movement. Second, 'off' q_γ currents were always simple monotonic decays rather than the complex waveforms reported earlier in cut fibres. Third, the q_γ 'on' and 'off' currents always decayed to stable baselines without the intervening inward transient phases or delayed outward currents reported earlier (Csernoch *et al.* 1991). Fourth, the 'on' q_γ 'humps', particularly prominent in such isolated transients, varied steeply with test voltage, but were always preceded by rapid charge transfers. Fifth, q_γ produced large rapid charge transfers similar to those of q_β decays at large depolarizations in contrast to the decline in q_γ amplitude reported in cut fibres at large depolarizations (Pizzaro *et al.* 1991). Sixth, the running integrals representing q_γ charge with time confirmed an 'on'–'off' charge equality under all these conditions whether test or prepulse voltage was varied. This contrasts with the relative deficit in 'off' q_γ charge reported in cut fibres (Szucs *et al.* 1991). All these features are consistent with a q_γ transition mediated by intramembrane capacitative charge as opposed to a hypothesis in which q_γ results from Ca^{2+} release.

Finally, the extracted q_γ currents, $I(t)$, were plotted against the corresponding charge, $Q(t)$, in the phase plane for the first time. This provided an empirical geometrical representation of the non-linear ordinary differential equations that might model q_γ charge (see Kreyszig, 1976; Jordan & Smith, 1987). The phase-plane trajectories, $I(Q)$, indicated that the charge movement, $I(t)$, varied both with the charge, $Q(t)$, at that time, t, and with test voltage, V. Thus, 'on' or 'off' steps imposed from a *fixed* prepulse level to *varying* test potentials gave declining phase-plane trajectories with topologies which varied markedly with the voltage and were of complex form in the 'on' responses. These findings would require the presence of at least one higher-order process described by kinetic terms that depended steeply and uniquely upon test voltage. Furthermore, the overall voltage dependence of such terms appeared to be autonomous of either time or previous charging history. Thus, 'on' or 'off' phase-plane plots derived from *varying* prepulse potentials to a *constant* test potential joined *similar* loci which ended at zero net charge movement. This suggests a single system with kinetics which are conserved with instantaneous charge distribution and voltage, in parallel with a similar conservation of its steady-state properties with voltage.

An involvement of two or more processes would have required them to have coincident voltage and charge dependences to maintain an overall $I(Q)$ conservation.

The actual form of the phase-plane plots suggests co-operative mechanisms that enhance 'on' q_γ charge following a prior monotonic current decay in a primarily capacitative process. These findings thus refine previous second-order models which predicted q_γ 'hump' currents but not the preceding decays (Huang, 1984, 1993*a*). Taken with the simpler 'off' plots, they could reflect the operation of a co-operative subunit system constrained into an associated (tense, T) resting form in fully polarized membrane (see Monod, Wyman & Changeux, 1965; Huang, 1983). A threshold depolarization might then elicit configurational changes in one or more such subunits and trigger a subsequent allosteric transition of the remaining assembly into a dissociated (relaxed, R) form with an accompanying delayed (q_γ) charge movement. In contrast, larger, suprathreshold 'on' steps could influence individual voltage-sensing subunits directly, as would 'off' voltage steps that would act upon subunits previously dissociated by the preceding 'on' step. Both the latter manoeuvres would elicit the observed monotonic current decays without prolonged phases or 'humps'.

Recent evidence suggests that transverse tubular dihydropyridine receptors, implicated in production of q_γ charge movement (Huang, 1990), form tetrad units in turn associated with sarcoplasmic reticular Ca^{2+}-release channels (Block, Imagawa, Campbell & Franzini-Armstrong, 1988). This offers a potential physical basis for such allosteric interactions (see Rios, Karhanek, Ma & Gonzalez, 1993), but only in a hypothesis in which q_γ is the electrical signature of configurational changes involved in the voltage-sensing and transduction events themselves, and not of the cytosolic Ca^{2+} release that is their consequence.

REFERENCES

Adrian, R. H. (1978). Charge movement in the membrane of striated muscle. *Annual Reviews of Biophysics and Bioengineering* **7**, 85–112.

Adrian, R. H. & Almers, W. (1974). Membrane capacity measurements on frog skeletal muscle in media of low ionic content. *Journal of Physiology* **237**, 573–605.

Adrian, R. H. & Almers, W. (1976). Charge movement in the membrane of striated muscle. *Journal of Physiology* **254**, 339–360.

Adrian, R. H. & Huang, C. L.-H. (1984). Charge movements near the mechanical threshold in skeletal muscle of *Rana temporaria*. *Journal of Physiology* **349**, 483–500.

Adrian, R. H. & Peres, A. (1979). Charge movement and membrane capacity in frog skeletal muscle. *Journal of Physiology* **289**, 83–97.

Block, B. A., Imagawa, T., Campbell, K. P. & Franzini-Armstrong, C. (1988). Structural evidence for direct interaction between the molecular components of the transverse tubular/sarcoplasmic reticulum junctions in skeletal muscle. *Journal of Cell Biology* **107**, 2587–2600.

Brum, G. & Rios, E. (1987). Intramembrane charge movement in frog skeletal muscle fibres. Properties of Charge 2. *Journal of Physiology* **387**, 489–517.

Chandler, W. K. & Hui, C. S. (1990). Membrane capacitance in frog cut twitch fibres mounted in a double vaseline-gap chamber. *Journal of General Physiology* **96**, 225–256.

Chandler, W. K., Rakowski, R. F. & Schneider, M. F. (1976). A non-linear voltage-dependent charge movement in frog skeletal muscle. *Journal of Physiology* **254**, 243–283.

Chen, W. & Hui, C. S. (1991). Gluconate suppresses Q_β more effectively than Q_γ in frog twitch fibers. *Biophysical Journal* **59**, 543a.

Csernoch, L., Pizarro, G., Uribe, I., Rodriguez, M. & Rios, E. (1991). Interfering with calcium release suppresses I_γ, the hump component of intramembranous charge movement in skeletal muscle. *Journal of General Physiology* **97**, 845–884.

Garcia, J., Pizarro, G., Rios, E. & Stefani, E. (1991). Effect of the calcium buffer EGTA on the 'hump' component of charge movement in skeletal muscle. *Journal of General Physiology* **97**, 885–896.

Huang, C. L.-H. (1981). Dielectric components of charge movements in skeletal muscle. *Journal of Physiology* **313**, 187–205.

Huang, C. L.-H. (1982). Pharmacological separation of charge movement components in frog skeletal muscle. *Journal of Physiology* **324**, 375–387.

Huang, C. L.-H. (1983). Time domain spectroscopy of the membrane capacitance in frog skeletal muscle. *Journal of Physiology* **341**, 1–24.

Huang, C. L.-H. (1984). Analysis of 'off' tails of intramembrane charge movements in skeletal muscle of *Rana temporaria*. *Journal of Physiology* **356**, 375–390.

Huang, C. L.-H. (1990). Voltage-dependent block of charge movement components by nifedipine in frog skeletal muscle. *Journal of General Physiology* **96**, 535–558.

Huang, C. L.-H. (1991). Separation of intramembrane charging components in low calcium solutions in frog skeletal muscle. *Journal of General Physiology* **98**, 249–264.

Huang, C. L.-H. (1993*a*). Intramembrane charge movements in striated muscle. *Monographs of the Physiological Society*, pp. 1–292. Clarendon Press, Oxford, UK.

Huang, C. L.-H. (1993*b*). Charge inactivation in the membrane of intact frog striated muscle fibres. *Journal of Physiology* **468**, 107–124.

Huang, C. L.-H. (1994). Charge conservation in intact frog skeletal muscle fibres in gluconate-containing solutions. *Journal of Physiology* **474**, 161–171.

Huang, C. L.-H. & Peachey, L. D. (1989). Anatomical distribution of voltage dependent membrane capacitance in frog skeletal muscle fibers. *Journal of General Physiology* **93**, 565–584.

Hui, C. S. (1983). Differential properties of two charge components in frog skeletal muscle. *Journal of Physiology* **337**, 531–552.

Hui, C. S. (1991). Factors affecting the appearance of the hump charge movement in frog cut twitch fibers. *Journal of General Physiology* **98**, 315–347.

Hui, C. S. & Chandler, W. K. (1990). Intramembranous charge movement in frog cut twitch fibers mounted in a double vaseline-gap chamber. *Journal of General Physiology* **96**, 257–297.

Hui, C. S. & Chandler, W. K. (1991). Q_β and Q_γ components of intramembranous charge movement in frog cut twitch fibers. *Journal of General Physiology* **98**, 429–464.

Hui, C. S. & Chen, W. (1992). Separation of Q_β and Q_γ charge components in frog cut twitch fibers with tetracaine. Critical comparison with other methods. *Journal of General Physiology* **99**, 985–1016.

Irving, M., Maylie, J., Sizto, N. L. & Chandler, W. K. (1987). Intrinsic optical and passive electrical properties of cut frog twitch fibers. *Journal of General Physiology* **89**, 1–40.

Irving, M., Maylie, J., Sizto, N. L. & Chandler, W. K. (1989). Simultaneous monitoring of changes in magnesium and calcium concentrations in frog cut twitch fibers containing antipyrylazo III. *Journal of General Physiology* **93**, 585–608.

Jong, D. S., Pape, P. C. & Chandler, W. K. (1992). Effects of sarcoplasmic reticulum calcium depletion on intramembranous charge movement in frog cut muscle fibers. *Biophysical Journal* **61**, A130.

Jordan, D. W. & Smith, P. (1987). *Nonlinear Ordinary Differential Equations*, pp. 1–381. Clarendon Press, Oxford, UK.

Kreyszig, E. (1976). *Advanced Engineering Mathematics*. John Wiley, New York.

Melzer, W., Schneider, M. F., Simon, B. J. & Szucs, G. (1986). Intramembrane charge movement and calcium release in frog skeletal muscle. *Journal of Physiology* **373**, 481–511.

Monod, J., Wyman, J. & Changeux, J. P. (1965). On the nature of allosteric transitions: a plausible model. *Journal of Molecular Biology* **12**, 88–118.

Pape, P. C., Jong, D. S. & Chandler, W. K. (1992). Effects of sarcoplasmic reticulum calcium loading on intramembranous charge movement in frog cut muscle fibers. *Biophysical Journal* **61**, A130.

Pizarro, G., Csernoch, L., Uribe, I., Rodriguez, M. & Rios, E. (1991). The relationship between Q_γ and Ca release from the sarcoplasmic reticulum in skeletal muscle. *Journal of General Physiology* **97**, 913–947.

Rios, E., Karhanek, M., Ma, J. & Gonzalez, A. (1993). An allosteric model of the molecular interactions of excitation-contraction coupling in skeletal muscle. *Journal of General Physiology* **102**, 449–481.

Szucs, G., Csernoch, L., Magyar, J. & Kovacs, L. (1991). Contraction threshold and the 'hump' component of charge movement in frog skeletal muscle. *Journal of General Physiology* **97**, 897–911.

Acknowledgements

The author thanks Mr W. Smith for skilled assistance and the Royal Society for partial equipment support.

Received 24 December 1993; accepted 4 April 1994.